



Asian Journal of Pharmaceutical Analysis and Medicinal Chemistry

Journal home page: www.ajpamc.com

<https://doi.org/10.36673/AJPAMC.2022.v10.i01.A05>



SYNTHESIS AND REACTIONS OF SOME NEW QUINAZOLINE DERIVATIVES FOR *IN VITRO* EVALUATION AS ANTICANCER AGENTS

T. Rashmi*¹ and T. Pramila¹

¹*Department of Pharmaceutical Chemistry, Bharathi College of Pharmacy, Bharathinagara, Maddur Taluk, Mandya, Karnataka, India.

ABSTRACT

Two new synthesized and characterized quinazoline Mannich bases 1 and 2 were investigated for anticancer activity against MCF-7 human breast cancer cell line. Compounds 1 and 2 demonstrated a remarkable anti-proliferative effect, with an IC_{50} value of 6.035×10^{-6} mol/L and 5.620×10^{-6} mol/L, respectively, after 72 hours of treatment. Most apoptosis morphological features in treated MCF-7 cells were observed by AO/PI staining. The results of cell cycle analysis indicate that compounds did not induce S and M phase arrest in cell after 24 hours of treatment. Furthermore, MCF-7 cells treated with 1 and 2 subjected to apoptosis death, as exhibited by perturbation of mitochondrial membrane potential and cytochrome c release as well as increase in ROS formation. We also found activation of caspases-3/7, -8 and -9 in compounds 1 and 2. Our results showed significant activity towards MCF-7 cells via either intrinsic or extrinsic mitochondrial pathway and are potential candidate for further *in vivo* and clinical breast cancer studies.

KEYWORDS

Quinazoline, Secondary amines and Anti-cancer activity.

Author for Correspondence:

Rashmi T,
Department of Pharmaceutical Chemistry,
Bharathi College of Pharmacy,
Maddur, Mandya, Karnataka, India.

Email: rashmitpharm@gmail.com

INTRODUCTION

Quinazoline nucleus is an interesting molecule among the most important classes of an aromatic bicyclic compounds with two nitrogen atoms in their structure. It is consisting of aromatic benzopyrimidine system made up of two fused six member simple aromatic rings benzene and pyrimidine ring¹ Figure No.1.

Recently, many efforts have been focused by chemists on the modification of quinazoline ring for development of pharmaceutical and clinical

compounds². A brief survey about biological importance of quinazoline and their derivatives revealed that a large number of publications began to appear after 1960s. Most of quinazoline derivatives which have been identified consist of wide range of biological and pharmaceutical activities such as anticancer³, antioxidant⁴, antiviral⁵, anticonvulsant⁶, anti-inflammatory⁷, antitubercular⁸, anti-HIV⁹, analgesic¹⁰ and antimicrobial¹¹. In addition, several studies have been conducted to evaluate the pharmacokinetics and toxicity of new quinazoline-based compounds in different animal model to prove the safe nature of their synthesized compounds^{12,13}.

Quinazoline is a compound made up of two fused six membered simple aromatic rings, a benzene ring and a pyrimidine ring. Its chemical formula is C₈H₆N₂. Quinazoline is yellow and amorphous. Any derivative of quinazoline may be described as quinazoline analogues. The derivatives were found with other activities like insecticidal and analgesic⁷. Quinazolines and condensed quinazolines are reported to show potent cytotoxic, antimicrobial and anti-HIV activities. The Position 2, 6 and 8 of this nucleus is very important for structural activity studies and 2, 3 disubstituted quinazolines are reported to possess antiviral, antihypertensive and antibacterial functions.

Cancer still is a major threat to human beings around the world. Among all diagnosed cancers, breast cancer is the second leading cause of death in women which is diagnosed in nearly 30% of all women in the United States^{14,15}. Normal cell typically dies through apoptosis which regulate cell proliferation and destruction of aberrant cells, however; in cancer cells, apoptosis is suppressed and required to be triggered which is a key factor in area of anticancer drug development¹⁶. Among all targets of cancer research, reactive oxygen species (ROS) play an important role in anticancer drug research. Since, generation of excessive ROS will result in perturbation of the mitochondrial membrane potential and release of cytochrome c from mitochondria in to the cytosol and consequently activates caspase-9 expression followed by activation of executioner caspases

including caspases-3 and -7 which induce execution phase of apoptosis¹⁷. Furthermore, activation of caspase-8 is closely involved in extrinsic signaling pathway of apoptosis¹⁸ which associated with inhibition of NF- κ B translocation¹⁹. If the activity of this factor is blocked, tumor cells can undergo apoptosis²⁰.

Although the current anticancer quinazoline-based agents have demonstrated great clinical benefits in cancer treatment²¹, we still need to establish better anticancer agents from quinazoline derivatives with minimum adverse side effects²² that provides much more hope to mankind. We are particularly interested in the present work to develop potential anticancer agents against breast cancer cell line and screen for their possible mechanism either intrinsic or extrinsic mitochondrial pathway. Therefore, we investigated anticancer potential of 9, 11-dibromo-6-methyl- 2H- [1, 2, 4, 5] tetrazino] [1, 6-C]quinazoline-3(4H)- thione-1-ethyl-piperidine (1) and 9, 11-dibromo-6-methyl- 2H- [1, 2, 4, 5] tetrazino] [1, 6- C]quinazoline-3(4H)- thione-1-ethyl-morpholine (2) Consequently, involved mechanism of apoptosis for the compounds was thoroughly examined.

EXPERIMENTAL SECTION

Reagent and chemicals

All chemicals and solvents used for synthesis of compounds were obtained from Merck and Sigma-Aldrich. Melting points of the synthesized compounds were determined by open capillary melting point apparatus and are uncorrected. Infrared spectra were obtained by using SHIMADZU FTIR 8400 spectrometer using potassium bromide pellet technique. UV-visible spectra were obtained with an Agilent Technologies Cary60 UV-VIS spectrophotometer; ¹H NMR spectra of the synthesized compounds were taken using BRUKER SPECTROSPIN-400MHz spectrometer using tetra methyl silane as an internal standard and deuterated DMSO was used as a solvent for NMR spectrophotometer and the chemical shift data were expressed as delta (δ) values related to TMS in ppm. The mass spectra of

the synthesized compounds were taken using GCMS-QP5050 SHIMADZU instrument.

General procedure for synthesis of quinazoline mannich bases

A series of quinazoline derivatives (1-15) were synthesized by condensing the basic quinazoline with secondary amines in presence of paraformaldehyde. The dark brown precipitate for (1) and yellow precipitates for (2) were formed during the reactions^{23,24}. Three-quarters of the solvent was evaporated and the precipitate was filtrated and washed with a cold ethanol and dried. The purity of the compounds was checked by melting point, TLC, IR, ¹H NMR, and mass spectroscopy.

Synthesis of 2, 4-disubstituted quinazoline derivatives involves the following steps -

Step 1: Synthesis of dibromoanthranilic acid

Anthranilic acid was dissolved in glacial acid and cooled below 15°C then bromine in acetic acid was added slowly to the anthranilic acid mixture till the reddish brown colour of the bromine persists. The product was filtered off and washed with benzene and it is then boiled with water containing HCl and filter hot under suction. Residue was extracted with boiling water, the filtrate upon cooling yield dibromoanthranilic acid.

Step 2: Acetylation of dibromoanthranilic acid

Anthranilic acid and acetic anhydride was taken in the ratio of 1:2M in a round bottomed flask. The reaction mixture was heated gently and refluxed for 1 hr. The excess acetic anhydride was distilled off. The reaction mixture was poured into beaker containing crushed ice, stirred constantly and filtered. The crude product was recrystallized from ethanol.

Step 3: Synthesis of thiocarbohydrazide

To a solution 0.05 M of hydrazine hydrate (10mL) in 95% ethanol (25mL), ammonium hydroxide (10mL) was added and the mixture was kept below 30°C and 4mL of carbon disulphide was added drop by drop slowly for a period of 20 min with stirring and the solution was allowed to stand on ice bath for half an hour. To this add 4.5g of sodium chloro acetate with stirring and finally on adding hydrazine hydrate 6mL immediate precipitate occurs and it is

filtered, washed with chloroform and recrystallised from methanol.

Step 4: Synthesis of 9, 11-dibromo-6-methyl-2H-[1, 2, 4, 5] tetrazino [1, 6-C] quinazoline-3(4H)-thione

An equimolar (0.01M) quantity of 5, 7-dibromo- 2-methyl-1, 3-benzoxazin- 4-one and thiocarbohydrazide a pinch of zinc chloride is fused by fusion method at a temperature of about 180°C.

Step 5: Synthesis of 4, 6-disubstitutedquinazoline derivatives

A mixture of appropriate quinazoline (0.01M), aromatic secondary amines (0.02M), paraformaldehyde (0.01M) in 20mL absolute ethanol containing HCl 0.5M is refluxed on a water bath for 3 hrs. The reaction mixtures are left over night and solid formed are collected. The completion of reaction was monitored by TLC.

Synthesis of 9, 11-dibromo-6-methyl- 2H- [1, 2, 4, 5] tetrazino][1, 6- C]quinazoline-3(4H)- thione-1-ethyl-piperidine (1) Figure No.3

According to above mentioned procedure. Yield: (2.55g, 98%); mp 236-238°C; characteristic IR data of (cm⁻¹): band stretching around 3050cm⁻¹ due to aromatic C-H stretching, strong N-H stretching band at 3433cm⁻¹, CH stretching of CH₂ and CH₃ group at 2941-2820cm⁻¹, C=N and C=C stretch at 1602cm⁻¹, C=S stretch at 1165cm⁻¹, CH bending of CH₂ and CH₃ at 1437-1467, C-Br at 721cm⁻¹ and substituted phenyl ring at 869cm⁻¹. ¹H NMR (400MHz, DMSO-*d*₆/TMS, ppm) of compound (1) shows sharp singlet at δ1.16, δ2.17-2.24 and δ2.61 accounting for CH₃, CH₂ and (CH₂)₃. The 2 protons of aromatic and 1 proton of NH appeared as multiplet at δ7.54-8.43. Further molecular ion peak at 490m/z confirmed its molecular weight.

Synthesis of 9,11-dibromo-6-methyl- 2H-[1,2,4,5] tetrazino][1,6- C]quinazoline-3(4H)- thione-1-ethyl-morpholine (2) Figure No.4

According to above mentioned procedure. Yield: (1.99 g, 86%); IR spectrum of compound (2) derivative illustrated band stretching around 3103cm⁻¹ due to aromatic C-H stretching, strong N-H stretching band at 3430cm⁻¹ and 1609 cm⁻¹ accounting for C=N and C=C stretch, C-O-C at 1101cm⁻¹, C=S stretch at 1165cm⁻¹, CH bending of

CH₂ and CH₃ at 2941-2820, C-Br at 721cm⁻¹ and substituted phenyl ring at 869cm⁻¹. ¹H NMR of compound 2 derivative showed sharp singlet at δ1.89, δ2.142-2.38 and δ8.95 accounting for CH₃, CH₂ and (CH₂)₃ respectively. The 4 protons of (CH₂O)₂ appeared as singlet at δ3.69. The 2 protons of aromatic and 1 proton of NH appeared as singlet at δ6.94-8.37 which confirmed the structure of the compound 2. Further molecular ion peak Figure No.9 at 491m/z and other prominent peaks at 431, 373, 327 and 260 confirmed its molecular weight.

MTT Cytotoxicity assay

The normal MCF-10 breast cells, normal WRL-68 hepatic cells, and human MCF-7 breast adenocarcinoma cells were obtained by National cancer institute, (NCI), Adyar, Chennai, India. Cytotoxicity test was performed using MTT (3-[4,5-dimethylthiazol-2-yl]-2,5-diphenyl tetrazoliumbromide) assay²⁵. Briefly, cells (5 × 10⁴ cells/mL) were seeded into 96-well sterile plates. On the next day, cells were treated with different concentrations of (1), (2) and doxorubicin as a positive control. After 24, 48 and 72 hours of incubation, we stained the incubated cells with 20 μL of MTT (0.121 × 10⁻⁶ mol/L) for 3 hours, and then 100 μL of DMSO was added to dissolve the resulting dark forazan crystals and incubated in dark for 2 hours. Finally, absorbance was measured at 570nm wavelength using ELISA reader (Hidex, Turku, Finland). The IC₅₀ value was calculated and data was reported as the average of three replicates.

LDH release assay

Cytotoxicity effect of the quinazoline-based compound was also assessed by performing a LDH (lactate dehydrogenase) release assay²⁶. In brief, MCF-7 cells were treated with (1) and (2) at different concentrations for 48 hours, the supernatant of the treated cells was transferred into 96-well plates, and then 100 μL of the LDH reaction solution (Pierce TM LDH Cytotoxicity Assay Kit, Thermo Scientific, Pittsburgh, PA) was added. After 30 minutes, the intensity of red colour in the samples presenting the LDH activity was measured at 490nm using a Tecan Infinite 200 Pro (Tecan, Mannedorf, Switzerland) microplate reader.

Morphological study

A combination of a cell-permeable DNA-binding dye, that is, acridine orange (AO) with plasma membrane-impermeable and DNA-binding dye propidium iodide (PI) was used to assess the morphological changes in treated MCF-7 cells²⁷. Briefly, MCF-7 cells were plated at a concentration of 1 × 10⁶ cell/mL and treated with (1) and (2) at different IC₅₀ value for 3 incubation periods (24, 48, and 72 hours). Moreover, untreated cells also were employed as normal control. Next, plates were incubated in an atmosphere of 5% CO₂ at 37°C. The cells were then centrifuged at 300 × g for 10 minutes and washed twice with cold phosphate buffered saline (PBS). Finally, we stained the cells with equal volume of a mixture of AO/PI (0.107 × 10⁻⁶ mol/L) and observed under a UV-fluorescent microscope (Olympus BX51) within 30 minutes before the fluorescence colour started to fade. Cell morphological assessment was carried out for features such as membrane blebbing, chromatin condensation, and other features of apoptosis.

Cell cycle analysis

Cellomics Cell Cycle kit 1 (Thermo Scientific, Pittsburgh, PA) was used for analyzing the cell cycle distribution induced by the quinazoline-based compounds²⁸. BrdU and phosphohistone H3 dyes are used for simultaneous quantification of nuclear DNA content to distinguish DNA replication in S phase cells and mitosis marker in M phase cells, respectively. Briefly, MCF-7 cells (1 × 10⁴ cells/well) were treated with different concentration of compounds or DMSO (negative control) for 24 hours. After fixing and staining the cells for BrdU and phosphohistone H3 for 30 minutes as described by the manufacturers protocols, we analysed the cells using a Cellomics Array Scan HCS reader (Thermo Scientific) and quantified the results using a Target Activation Bioapplication module.

Reactive Oxygen Species (ROS) Assay

The generation of intra cellular ROS induced by quinazoline-based compounds was measured using a Cellomics Oxidative Stress1 HCS Reagent Kit (Thermo Scientific, Pittsburgh, PA), according to the manufacturers protocols^{29,30}. In response to oxidative stress and production of reactive oxygen

species (ROS), Dihydroethidium (DHE) dye reagent is converted to fluorescent ethidium and intercalates into DNA. In brief, MCF-7 cells were treated with (1) and (2) at different concentrations for 24 hours. DHE dye was then added to the treated cells and incubated for 30 minutes. Next, cells were fixed and washed with the wash buffer provided with the kit. Finally, the fluorescence intensity reflected the oxidation of the DHE dye to ethidium, which allowed for the measurement of the ROS generation using a fluorescent plate reader at an excitation wavelength of 520nm and an emission wavelength of 620nm.

Multiple Cytotoxicity Assay

Cellomics Multiparameter Cytotoxicity 3 Kit was used as previously described by Arbab, *et al*³¹. This kit enables to analyze crucial apoptotic events, including the loss of cells, changes in cell permeability, cytochrome c release, changes in mitochondrial membrane potential (MMP), morphological features, and nuclear size. Apoptotic events indicated above in the MCF-7 cells after treatment with the quinazoline-based compounds were simultaneously measured. An ArrayScan High Content Screening (HCS) system was used to analyze the stained cells in the plates (Cellomics, PA, USA).

Caspases-3/7, -8, and -9 Activity Assay

Caspase-Glo 3/7, 8, and 9 kit (Promega, Madison, WI) was used to determine the activation of caspases-3/7, -8, and -9³². In brief, the MCF-7 cells were seeded into a white-walled 96-well plate and treated with the different concentrations of (1) and (2) for 24 hours. After adding 100 μ L of Glo 3/7, 8, and 9 reagents and incubating for 30 minutes in room temperature, the activity of the caspases in the treated cells was measured as the degree of miniluciferin-labelled synthetic tetrapeptide cleavage and luciferase enzyme substrate release using a Tecan Infinite 200 Pro microplate reader (Tecan, Männedorf, Switzerland). Moreover, time-dependent manner experiment was also conducted to confirm the expression level of caspases and thus MCF-7 cells were treated with (1) and (2) with concentrations of 8.0×10^{-6} and 7.6×10^{-6} mol/L, respectively (Table

No.2). Then we examined the expression level of caspases-3/7, -8, and -9 in different times.

RESULTS AND DISCUSSION

MTT Cytotoxicity Assay

MTT cytotoxicity assay was performed to assess the anti-proliferation effect of both compounds on MCF-7 cancer cell. The result showed that compounds (1) and (2) significantly inhibited the proliferation of MCF-7 cells; however, they exhibited no suppressive activity against human normal MCF-10 breast cells and normal WRL-68 hepatic cells compared to IC₅₀ value of compounds toward MCF-7 cells. In this assay, IC₅₀ value of doxorubicin was also recorded as positive control, Table No.2.

LDH Cytotoxicity Assay

The cytotoxicity effect of the quinazoline-based compounds was also assessed by lactate dehydrogenase (LDH) release test on MCF-7 cells treated with different concentrations of (1) and (2) for 48 hours incubation. Both compounds induced significant cytotoxicity at concentrations of 4×10^{-6} , 8×10^{-6} and 16×10^{-6} mol/L and significantly increased the release of LDH in treated cells compared to control cells, Figure No.5. The significant levels of LDH release have been observed at a concentration of 8×10^{-6} and 16×10^{-6} mol/L.

Morphological Observation

Acridine Orange (AO) and Propidium Iodide (PI) excite, respectively, green and orange fluorescent under fluorescent microscope when they are intercalated into DNA. Late apoptotic and necrotic cells can take both AO and PI; however, viable and early apoptotic cells can stain only by AO²⁷. Morphological changes of (1) and (2) treated MCF-7 cell were examined after 24 and 48 h treatment with IC₅₀ values shown in Table No.2. Cell morphological assessment showed the effects of compounds to be more prominent in treated MCF-7 cells when compared to untreated cells, Figure No.6.

The untreated MCF-7 cells exhibited green healthy intact nuclei. After 24 hours of treatment, chromatin condensation and membrane blebbing (indicated by

small protrusions of the membrane) are most significant features of early apoptotic events. These characteristics were more pronounced at 48 hours of treatment, which was associated with the presence of orange colour as a result of the PI-positive band of denaturated DNA. In addition, the presence of secondary necrosis was more prominent, as the prolonged incubation of treated MCF-7 cells might induce secondary necrosis following the late apoptosis. Morphological changes of treated MCF-7 cells indicated the induction of apoptosis by selected quinazoline-based compounds. The criteria of cell morphology identification are as follows: green intact nucleus, viable cells; dense green areas of chromatin condensation in the nucleus, early apoptosis; dense orange areas of chromatin condensation, late apoptosis; and orange intact nucleus, secondary necrosis.

(a) Untreated MCF-7 cells exhibit normal structures. (b1) and (c1) Early apoptosis features, namely, blebbing and chromatin condensation as well as late apoptotic cells, were detected after 24 h of treatment with (1) and (2). (b2) and (c2) Late apoptosis and secondary necrosis were observed after 48 h of treatment with (1) and (2), respectively. (Magnification: 200x). VI: viable cells; CC: chromatin condensation; BL: blebbing of the cell membrane; LA: late apoptosis; SN: necrosis.

Cell Cycle Analysis

Cell cycle distribution was also investigated to test if (1) and (2) cause a cell cycle stage-inhibition²⁸. The images of cell-stained with BrdU and phosphohistone H3 showed no significant difference between treated cells and untreated cells for both quinazoline compounds

[Figure No.7(a)]. The intensities of (1) and (2) treated and untreated MCF-7 cells indicated that the level of BrdU and phosphohistone H3 intensities were reduced [Figure No.7(b)]. These results indicate that compounds did not induce S/M phases arrest in MCF-7 after 24 hours of treatment.

Figure No.7: Cell cycle analysis. (a) Effect of (1) and (2) on cell cycle arrest. After incubation with DMSO or different concentrations of (1) and (2) for 24 h, MCF-7 cells were stained with BrdU and

phosphohistone H3 and subjected to the Cellomics Array Scan HCS reader for cell cycle analysis. (b) Representative bar charts indicating that treatment of both compounds markedly decreased BrdU and phosphohistone H3 fluorescence intensities in treated MCF-7 cells. Data were expressed as the mean \pm SD of fluorescence intensity readings for three independent experiments.

Measurement of Reactive Oxygen Species (ROS)

Upgrading in the level of ROS or/and reduction in the level of antioxidants can trigger mitochondrial-initiated events leading to apoptosis^{29,30}. Furthermore, production of ROS can disrupt the homeostasis in the enzyme system of ROS scavenging antioxidants. Generation of ROS was measured in the treated MCF-7 cells with different concentrations of (1) and (2). Exposure to the quinazoline-based compounds caused the significant production of ROS in the treated MCF-7 cells, 2-fold higher than normal control, at 4×10^{-6} , 8×10^{-6} and 16×10^{-6} mol/L concentrations after 24 hours, Figure No.8.

Mitochondria-Initiated Events Analysis

There are convincing evidences that ROS may contribute to cytochrome c release due to disruption of the mitochondrial membrane potential³¹. In the present study, the MMP fluorescent probe was applied to assess the function of mitochondria. As shown in Figure No.9(a), untreated cells revealed maximal dye uptake, while the treated cells with (1) and (2) were very slightly stained after 24 hours. Decline in MMP fluorescent intensities indicated that the MMP is reduced in the treated cells with 4×10^{-6} , 8×10^{-6} , and 16×10^{-6} mol/L concentrations. In contrast, a significant elevation in cell membrane permeability was also observed at the same concentration after 24 hours exposure of MCF-7 cells to the quinazoline based compounds. Moreover, the release of cytochrome c from mitochondria to cytosol increased significantly compared to the control cells after 24 hours which is closely associated with the activity of ROS, Figure No.9(b).

Figure No.9: Effects of the Quinazoline Mannich bases on nuclear morphology, membrane permeability, mitochondrial membrane potential

(MMP), and cytochrome c release. (a) Representative images of MCF-7 cells treated with medium alone and at 4×10^{-6} , 8×10^{-6} and 16×10^{-6} mol/L concentrations of compounds and stained with Hoechst 33342 for nuclear, cytochrome c, membrane permeability and MMP dyes. Both compound induced a noteworthy elevation in membrane permeability and cytochrome c release and a marked reduction in mitochondrial membrane potential (magnification: 200x).

(b) Representative bar charts indicating dose-dependent increased cell permeability reduced MMP and increased cytochrome c release in treated MCF-7 cells.

Caspases-3/7, -8, and -9 activation analysis

Induction of apoptosis is precisely mediated by caspases cascade via both intrinsic and extrinsic pathway. Caspases play essential role in apoptosis which mainly included two main groups of initiators and executioners³². Caspases-8 and -9 are known as initiator caspases through extrinsic and intrinsic pathway, respectively and facilitate the activation of executioners, such as caspases-3/7.

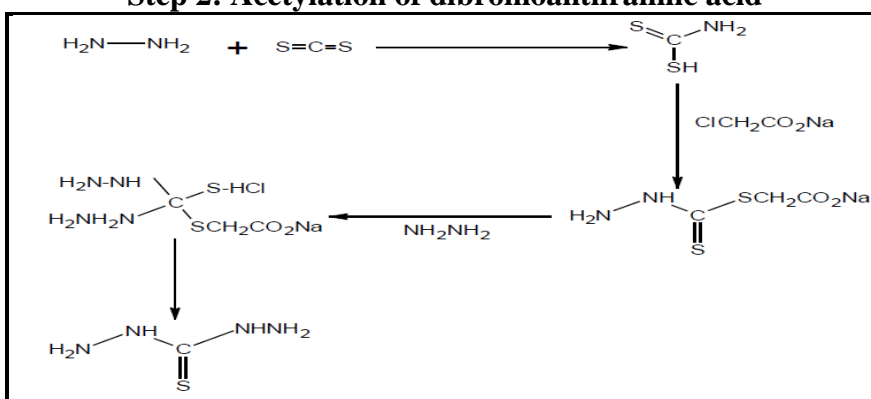
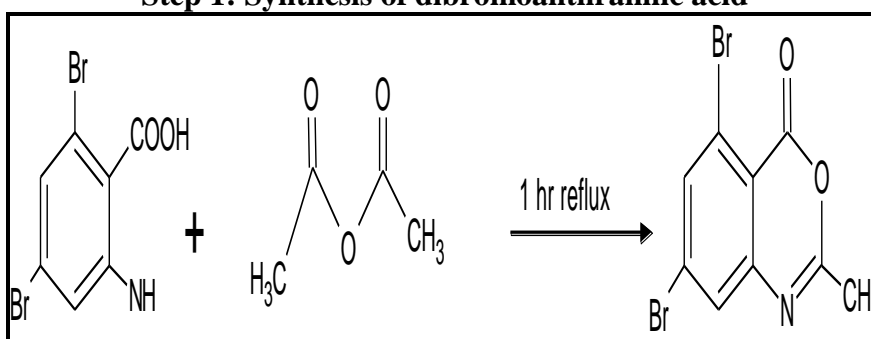
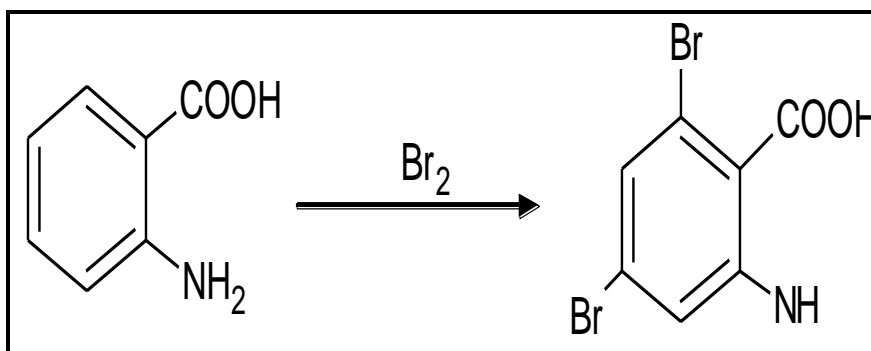
Therefore, the bioluminescent intensities of respective caspases presenting their activities were measured time-dependently in MCF-7 cells treated with different concentrations of (1) and (2) for 24 hours treatment. As shown in Figure No.10, compound (1) induced significant expression of caspases-8, -9, and -3/7 activities in MCF-7 treated cells at 8.0×10^{-6} mol/L in different times. Meanwhile, at 7.6×10^{-6} mol/L, (2) induced high expression level of caspases- 9 and -3/7 activities for different time; however, caspase-8 did not reveal any considerable activation in comparison to untreated cells. Thus, (1) induced apoptosis in MCF-7 via both intrinsic and extrinsic pathway; however, (2) was able to induce apoptosis only through mitochondria with high expression of caspase-9.

Table No.1: Substitutions of derivative (1-15)

Compound	Z
1	Piperidine
2	Morpholine
3	Diethylamine
4	Dimethylamine
5	Diphenylamine
6	Dibutylamine
7	Dibenzylamine
8	Pyrolidine
9	Propylamine
10	Piperazine
11	Phenyl Piperazine
12	Dihexylamine
13	Dioctylamine
14	4-methyl- Piperazine
15	2-nitro-diphenylamine

Table No.2: The IC₅₀ concentration of the quinazoline-based compounds against MCF-7, MCF-10, and WRL-68 cell lines after 24, 48, and 72 h

Compound	Cell line	Classification	24 h	IC ₅₀ (μg/mL) 48 h	72 h
1	MCF-7	Breast cancer cells	8.053 X 10 ⁻⁶ mol/L	7.488 X 10 ⁻⁶ mol/L	6.035 X 10 ⁻⁶ mol/L
	MCF-10	Normal breast cells	0.481 X 10 ⁻⁶ mol/L	0.481 X 10 ⁻⁶ mol/L	0.481 X 10 ⁻⁶ mol/L
	WRL-68	Normal hepatic cells	0.751 X 10 ⁻⁶ mol/L	0.751 X 10 ⁻⁶ mol/L	0.751 X 10 ⁻⁶ mol/L
2	MCF-7	Breast cancer cells	7.505 X 10 ⁻⁶ mol/L	6.521 X 10 ⁻⁶ mol/L	5.620 X 10 ⁻⁶ mol/L
	MCF-10	Normal breast cells	0.481 X 10 ⁻⁶ mol/L	0.481 X 10 ⁻⁶ mol/L	0.481 X 10 ⁻⁶ mol/L
	WRL-68	Normal hepatic cells	0.751 X 10 ⁻⁶ mol/L	0.751 X 10 ⁻⁶ mol/L	0.751 X 10 ⁻⁶ mol/L
Doxorubicin	MCF-7	Breast cancer cells	4.271 X 10 ⁻⁶ mol/L	4.140 X 10 ⁻⁶ mol/L	3.507 X 10 ⁻⁶ mol/L



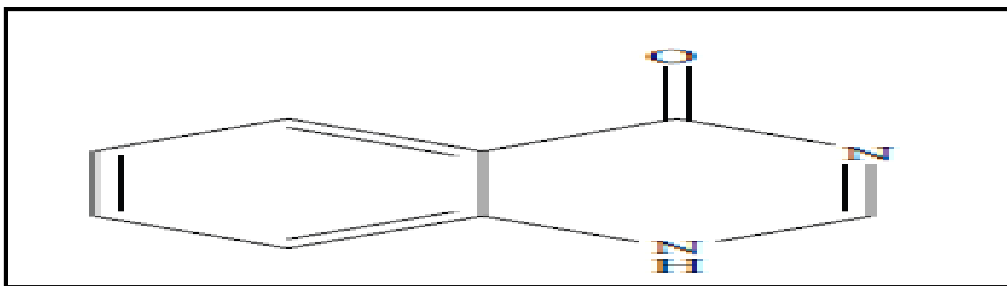


Figure No.1: Quinazoline-4-one

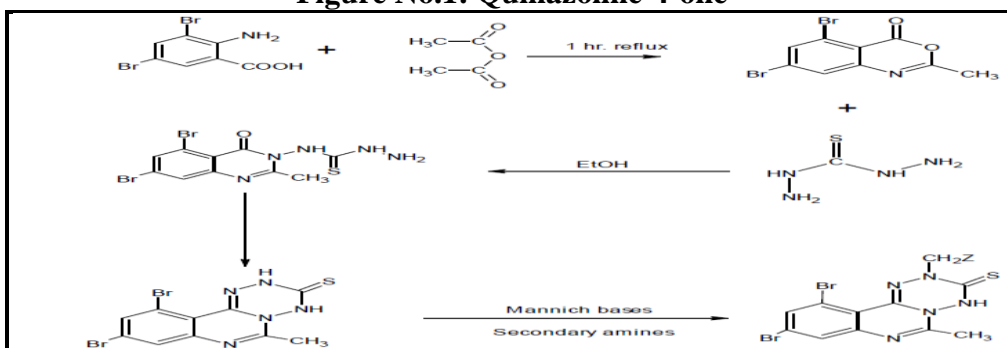


Figure No.2: Reaction scheme

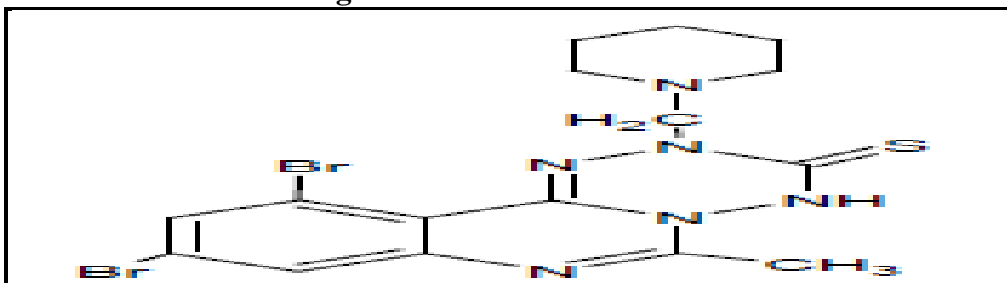


Figure No.3: Compound (1)

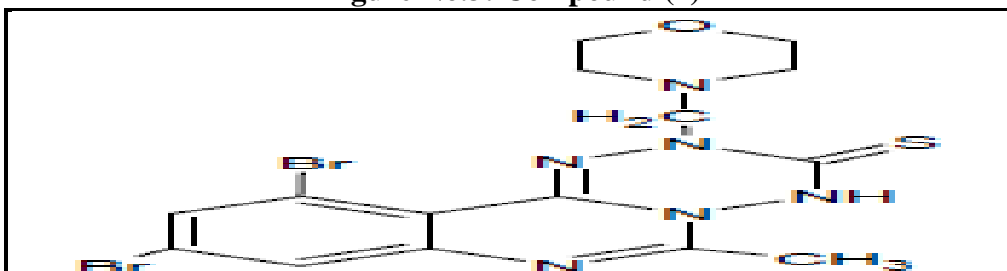


Figure No.4: Compound (2)

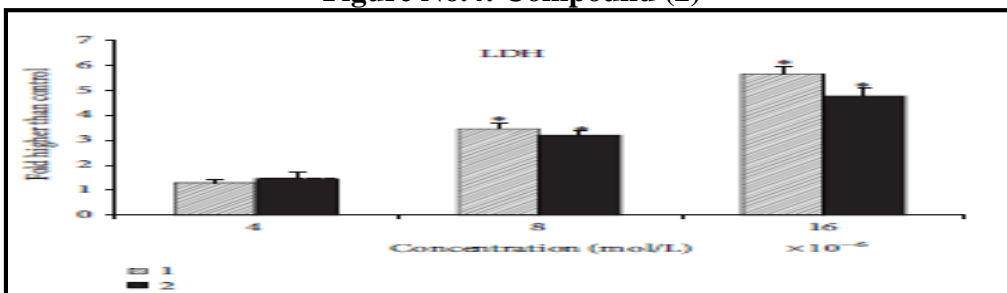


Figure No.5: The LDH release assay revealed the significant cytotoxicity of the quinazoline-based compound on MCF-7 cells at concentrations 4×10^{-6} , 8×10^{-6} , and 16×10^{-6} mol/L

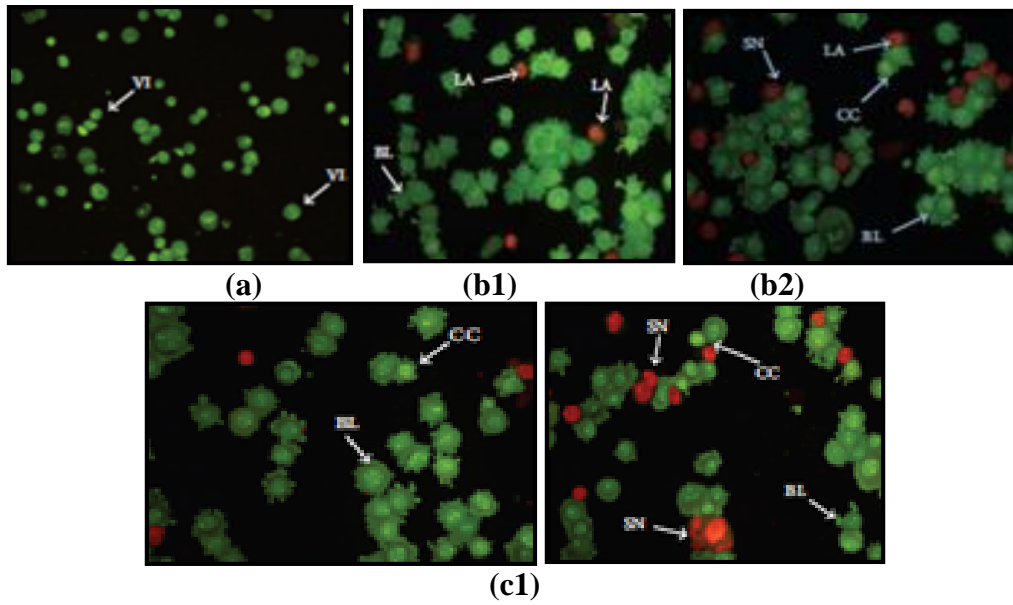


Figure No.6: Fluorescent micrographs of AO/PI-double-stained MCF-7 cells

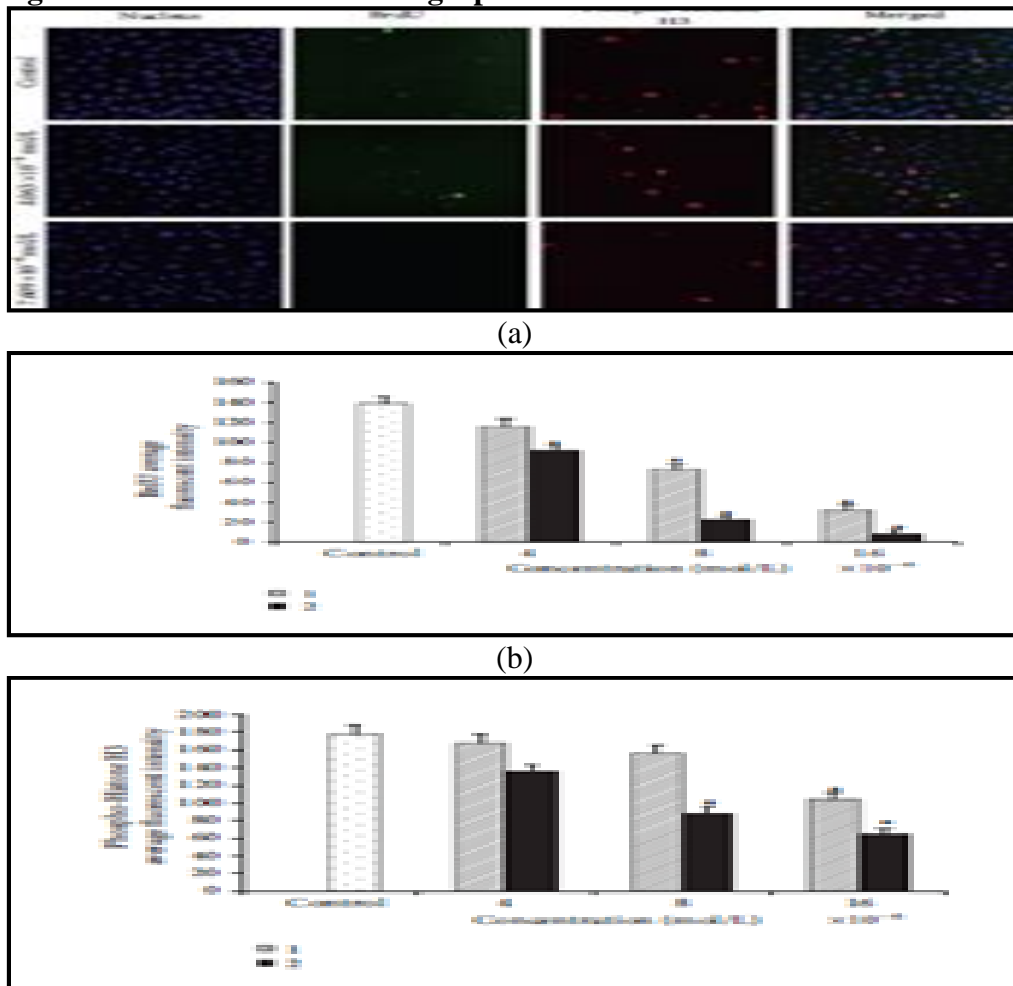


Figure 7: Cell cycle analysis. (a) Effect of (1) and (2) on cell cycle arrest. After incubation with DMSO or different concentrations of (1)

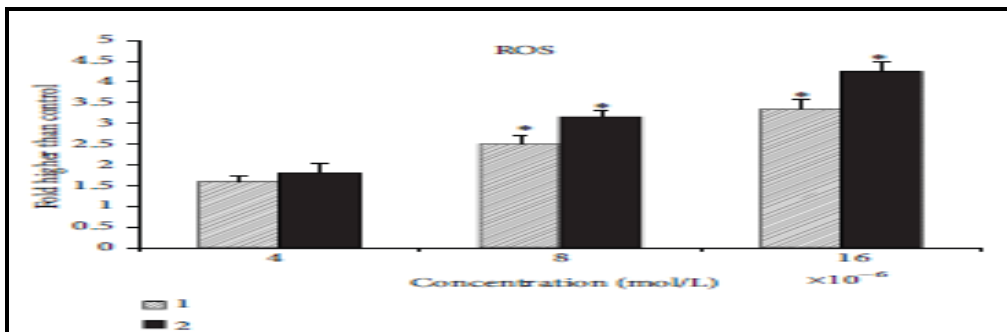
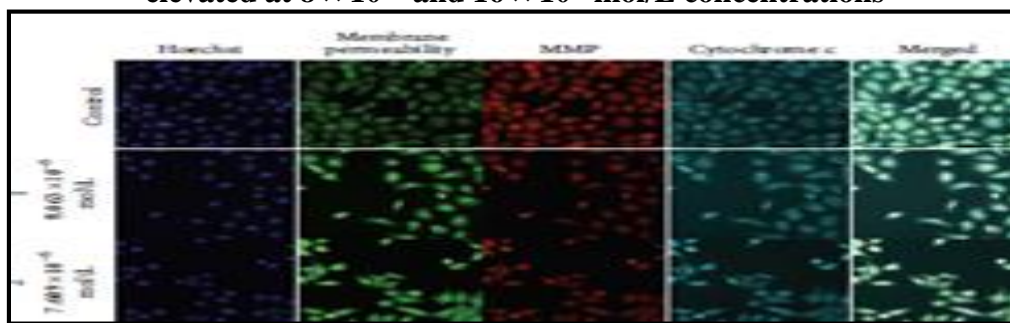
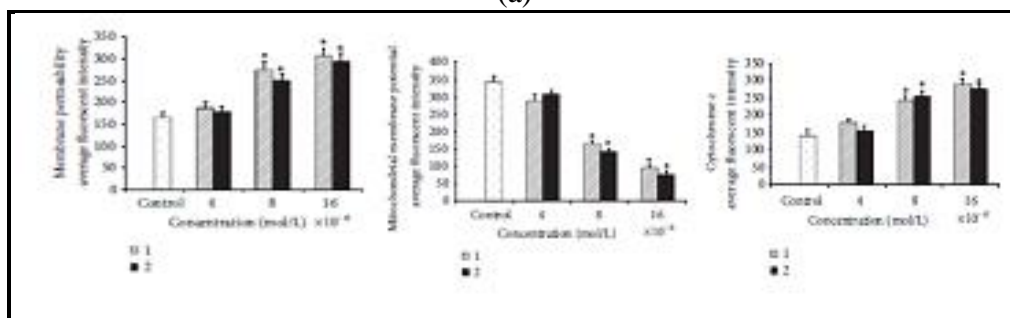


Figure No.8: Effect of MMD compound on the generation of ROS. The level of ROS significantly elevated at 8×10^{-6} and 16×10^{-6} mol/L concentrations

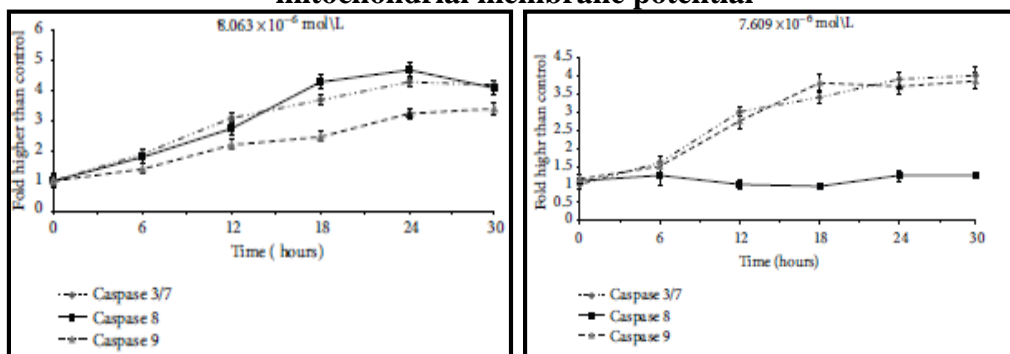


(a)



(b)

Figure 9: Effects of the Quinazoline Mannich bases on nuclear morphology, membrane permeability, mitochondrial membrane potential



(a)

(b)

Figure 10: Relative luminescence time-dependent expression of caspases-3/7, -8, and -9 in MCF-7 cells treated with (1) and (2) at concentrations of 8×10^{-6} mol/L and 7.6×10^{-6} mol/L, respectively, after 24 hours incubation

CONCLUSION

The synthesized quinazoline Mannich bases (1) and (2) established their structures by IR, NMR and mass spectroscopic studies. They have shown anticancer potential against MCF7 breast cancer cells. It was found out that compounds possess the capability of inducing intrinsic and extrinsic apoptosis pathway, which was well regulated by caspase enzymes. Moreover, the active role of mitochondria in the cell death was confirmed by reducing the MMP, release of cytochrome C and ROS elevation. Our results showed that compounds are promising anticancer agents. However, further research in the area of *in vivo* studies on the compounds might be vital for the development of new pharmaceuticals drugs.

ACKNOWLEDGEMENT

The authors thank the Rajiv Gandhi University of Health Sciences, Karnataka, Bengaluru, for rendering financial support (PROJECT CODE-P015 and ORDER NO. RGU/ADV.RES/BR/001/2017-18 DATED: 21.12.2017) and providing grant funding to conduct this study.

CONFLICT OF INTEREST

The authors declare that there is no conflict of interests regarding the publication of this paper.

BIBLIOGRAPHY

1. Bogentoft C, Kronberg L. Studies on the medicinal chemistry of oxoquinazolines IV N- and O-alkylation of some 2-substituted 3, 4-dihydro-4-oxoquinazolines, *Acta Pharmaceutica Suecica*, 6(4), 1969, 489-500.
2. Theivendren P S, Palanirajan V K. Quinazoline marketed drugs—A review, *Research in Pharmacy*, 1(1), 2011, 1-21.
3. Latli B, Wood E, Casida J E. Insecticidal quinazoline derivatives with (trifluoromethyl) diazirinyl and azido substituents as NADH: Ubiquinone oxidoreductase inhibitors and candidate photoaffinity probes, *Chemical Research in Toxicology*, 9(2), 1996, 445-450.
4. Vagdevi H M, Lokesh M R, Gowdarshivannanavar B C. Synthesis and antioxidant activity of 3-substituted Schiff bases of quinazoline-2, 4-diones, *Int J Chem Tech Res*, 4(4), 2012, 1527-1533.
5. Krishnan S K, Ganguly S, Veerasamy R, Jan B. Synthesis, antiviral and cytotoxic investigation of 2-phenyl-3-substituted quinazolin-4 (3H)-ones, *Eur Rev Med Pharmacol Sci*, 15(6), 2011, 673-681.
6. Patel N B, Patel V N, Patel H R, Shaikh F M, Patel J C. Synthesis and microbial studies of (4-oxo-thiazolidinyl) sulfonamides bearing quinazolin-4 (3H) ones, *Acta Poloniae Pharmaceutica: Drug Research*, 67(3), 2010, 267-275.
7. Alafeefy A M, Kadi A A, Al-Deeb O A, El-Tahir K E, Al-Jaber N A. Synthesis, analgesic and anti-inflammatory evaluation of some novel quinazoline derivatives, *European Journal of Medicinal Chemistry*, 45(11), 2010, 4947-4952.
8. Abid O H, Ahmed A H. Synthesis and characterization of novel quinazoline derivatives via reaction of isatoic anhydride with schiff's base, *International Journal of Applied and Natural Sciences*, 2(5), 2013, 11-20.
9. Pati B, Banerjee S. Quinazolines: An illustrated review, *Journal of Advanced Pharmacy Education and Research*, 3(3), 2013, 136-151.
10. Alagarsamy V, Muthukumar V, Pavalarani N, Vasanathan P, Revathi R. Synthesis, analgesic and anti-inflammatory activities of some novel 2, 3-disubstituted quinazolin-4 (3H)-ones, *Biological and Pharmaceutical Bulletin*, 26(4), 2003, 557-559.
11. Sumathy A, Karthik D, Palanisamy S. A study on synthesis, molecular properties and antimicrobial activity of some quinazoline derivatives, *Journal of Chemical and Pharmaceutical Research*, 5(10), 2013, 1-9.
12. Trieu V N, Liu X P, Chen C L, Uckun F M. Treatment of atherosclerosis in apolipoprotein E-deficient mice with 4-(3'-bromobenzoyl)-6,

- 7-dimethoxyquinazoline (WHI-P164), a potent inhibitor of triglyceride synthesis, *Journal of Cardiovascular Pharmacology*, 35(2), 2000, 179-188.
13. Uckun F M, Ek O, Liu X P, Chen C L. *In vivo* toxicity and pharmacokinetic features of the janus kinase 3 inhibitor WHI-P131 [4-(4'-Hydroxyphenyl)-amino-6, 7-dimethoxyquinazoline], *Clinical Cancer Research*, 5(10), 1999, 2954-2962.
 14. Tan M L, Sulaiman S F, Najimuddin N, Samian M R, Muhammad T T. Methanolic extract of *Pereskia bleo* (Kunth) DC. (Cactaceae) induces apoptosis in breast carcinoma, T47-D cell line, *Journal of Ethnopharmacology*, 96(1-2), 2005, 287-294.
 15. Tanih N F, Ndip R N. The acetone extract of *Sclerocarya birrea* (Anacardiaceae) possesses antiproliferative and apoptotic potential against human breast cancer cell lines (MCF-7), *The Scientific World Journal*, 2013, Article ID: 956206, 2013, 201-203.
 16. Hunter A M, LaCasse E C, Korneluk R G. The inhibitors of apoptosis (IAPs) as cancer targets, *Apoptosis*, 12(9), 2007, 1543-1568.
 17. Simon H U, Haj-Yehia A, Levi-Schaffer F. Role of reactive oxygen species (ROS) in apoptosis induction, *Apoptosis*, 5(5), 2000, 415-418.
 18. Jin Z, Li Y, Pitti R, Lawrence D, Pham V C, Lill J R, Ashkenazi A. Cullin3-based polyubiquitination and p62-dependent aggregation of caspase-8 mediate extrinsic apoptosis signaling, *Cell*, 137(4), 2009, 721-735.
 19. Yang L Q, Fang D C, Wang R Q, Yang S M. Effect of NF- κ B, survivin, Bcl-2 and Caspase3 on apoptosis of gastric cancer cells induced by tumor necrosis factor related apoptosis inducing ligand, *World Journal of Gastroenterology*, 10(1), 2004, 22-25.
 20. Dalen H, Neuzil J. α -Tocopheryl succinate sensitises a T lymphoma cell line to TRAIL-induced apoptosis by suppressing NF- κ B activation, *British Journal of Cancer*, 88(1), 2003, 153-158.
 21. Selvam T P, Kumar P V. Quinazoline marketed drugs, *Research in Pharmacy*, 1(1), 2015, 1-21.
 22. Kranz D, Dobbelstein M. A killer promoting survival: p53 as a selective means to avoid side effects of chemotherapy, *Cell Cycle*, 11(11), 2012, 2053-2057.
 23. Li J, Meng Y, Liu Y, Feng Z Q, Chen X G. F84, a quinazoline derivative, exhibits high potent antitumor activity against human gynecologic malignancies, *Investigational New Drugs*, 28(2), 2010, 132-138.
 24. Bavetsias V, Marriott JH, Melin C, Kimbell R, Matusiak Z S, Boyle F T, Jackman A L. Design and synthesis of Cyclopenta [g] quinazoline-based antifolates as inhibitors of thymidylate synthase and potential antitumor agents, *Journal of Medicinal Chemistry*, 43(10), 2000, 1910-1926.
 25. Skehan P, Storeng R, Scudiero D, Monks A, McMahon J, Vistica D, Warren J T, Bokesch H, Kenney S, Boyd M R. New colorimetric cytotoxicity assay for anticancer-drug screening, *Journal of the National Cancer Institute*, 82(13), 1990, 1107-1112.
 26. Karimian H, Mohan S, Moghadamtousi S Z, Fadaeinasab M, Razavi M, Arya A, Kamalidehghan B, Ali H M, Noordin M I. *Tanacetum polycephalum* (L.) schultz-bip, induces mitochondrial-mediated apoptosis and inhibits migration and invasion in MCF7 cells, *Molecules*, 19(7), 2014, 9478-9501.
 27. Mascotti K, McCullough J, Burger S R. HPC viability measurement: Trypan blue versus acridine orange and propidium iodide, *Transfusion*, 40(6), 2000, 693-696.
 28. Mohan S, Abdelwahab SI, Kamalidehghan B, Syam S, May K S, Harmal N S, Shafifiyaz N, Hadi A H, Hashim N M, Rahmani M, Taha M M. Involvement of NF- κ B and Bcl2/Bax signaling pathways in the apoptosis of MCF7 cells induced by a xanthone compound Pyranocycloartobioxanthone A, *Phytomedicine*, 19(11), 2012, 1007-1015.
 29. Zamzami N, Marchetti P, Castedo M, Decaudin D, Macho A, Hirsch T, Susin S A,

Petit P X, Mignotte B, Kroemer G. Sequential reduction of mitochondrial transmembrane potential and generation of reactive oxygen species in early programmed cell death, *The Journal of Experimental Medicine*, 182(2), 1995, 367-377.

30. Simon H U, Haj-Yehia A, Levi-Schaffer F. Role of reactive oxygen species (ROS) in apoptosis induction, *Apoptosis*, 5(5), 2000, 415-418.
31. Mosmann T. Rapid colorimetric assay for cellular growth and survival: application to proliferation and cytotoxicity assays, *The Scientific World Journal 15 Journal of Immunological Methods*, 65(2), 1983, 53-63.
32. Arbab I A, Looi C Y, Abdul A B, Cheah F K, Wong W F, Sukari M A, Abdullah R, Mohan S, Syam S, Arya A, Mohamed Elhassan Taha M. Dentatin induces apoptosis in prostate cancer cells via Bcl-2, Bcl-xL, Survivin downregulation, caspase-9,-3/7 activation, and NF- κ B inhibition, *Evidence-Based Complementary and Alternative Medicine*, 2012, Article ID: 856029, 2012, 15.

Please cite this article in press as: Rashmi T and Pramila T. Synthesis and reactions of some new quinazoline derivatives for *in vitro* evaluation as anticancer agents, *Asian Journal of Pharmaceutical Analysis and Medicinal Chemistry*, 10(1), 2022, 29-42.